

Phase-Retrieval Wave-Front Sensing for the Hubble and Future Space Telescopes

James R. Fienup
Robert E. Hopkins Professor of Optics
University of Rochester
Institute of Optics

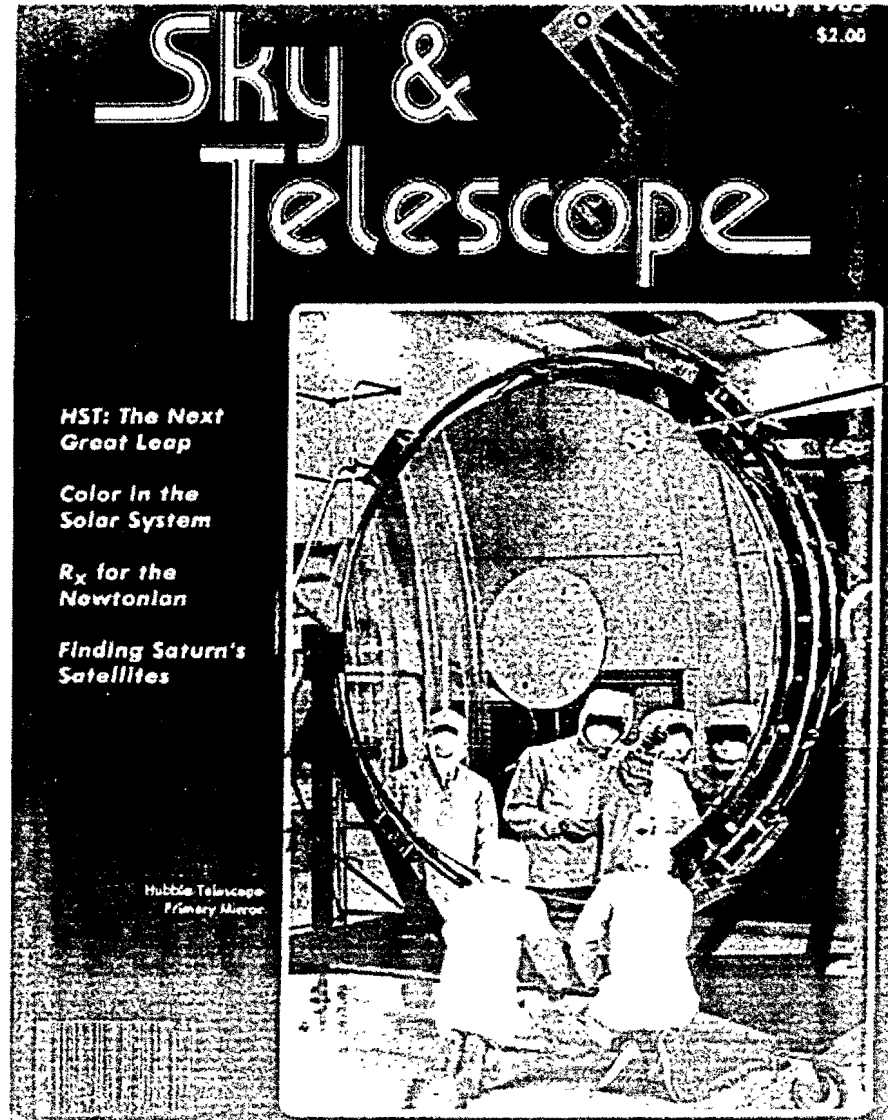
fienup@optics.rochester.edu

Presented at
XXXV Optical Society of India Symposium
on Contemporary Trends in Optics and Optoelectronics
17 January, 2011

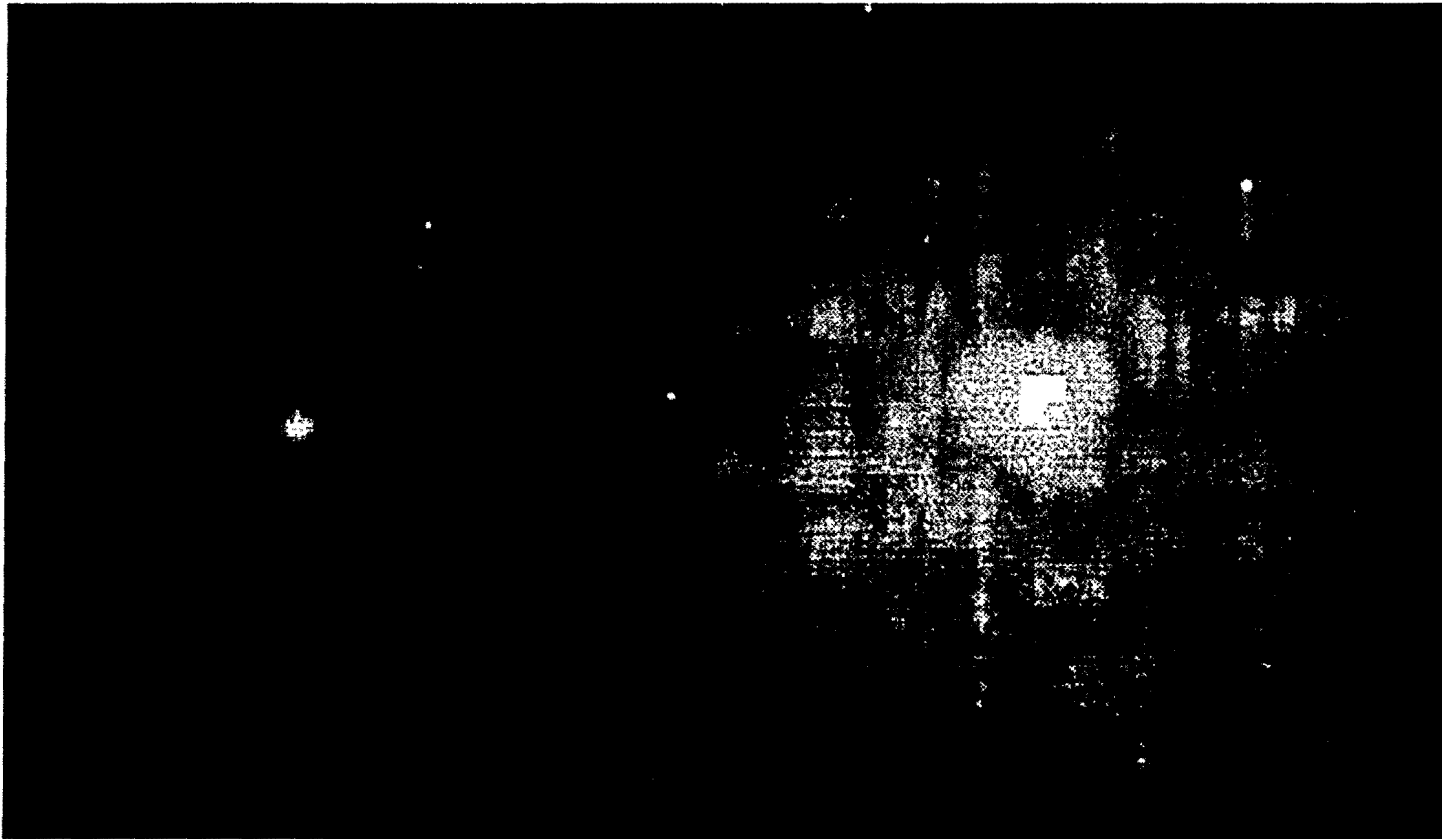
- Hubble Space Telescope (HST)
 - Problem needs fixing
 - Phase retrieval algorithms
 - Effect of phase retrieval on the prescription
 - HST Repaired
- James Webb Space Telescope (JWST)
 - Background: foldable, segmented-aperture telescope
 - Phase retrieval will be used for wavefront sensing and control

Jim Fienup was at ERIM, Ann Arbor, MI, during the HST recovery period

Hubble Space Telescope: Great Expectations, Pre-Launch



Note: Pads



Expected

Actual

Panels and Organizations Characterizing and Fixing HST

HST Optical System Board of Investigation
(Low Allen Committee)
How did it happen? Who was to blame?

HST Independent Optical
Review Panel (HIORP)
Characterize error to fix WF/PC2

(JRF, IPWG representative)

HST Strategy
Panel
How to fix HST
in general

HST Image Processing
Working Group (IPWG)
Improve imagery by post-
detection processing

(JRF, member)

Instrument Teams:
WF/PC, FOC,
HRS, FGS, ...
Vested interest

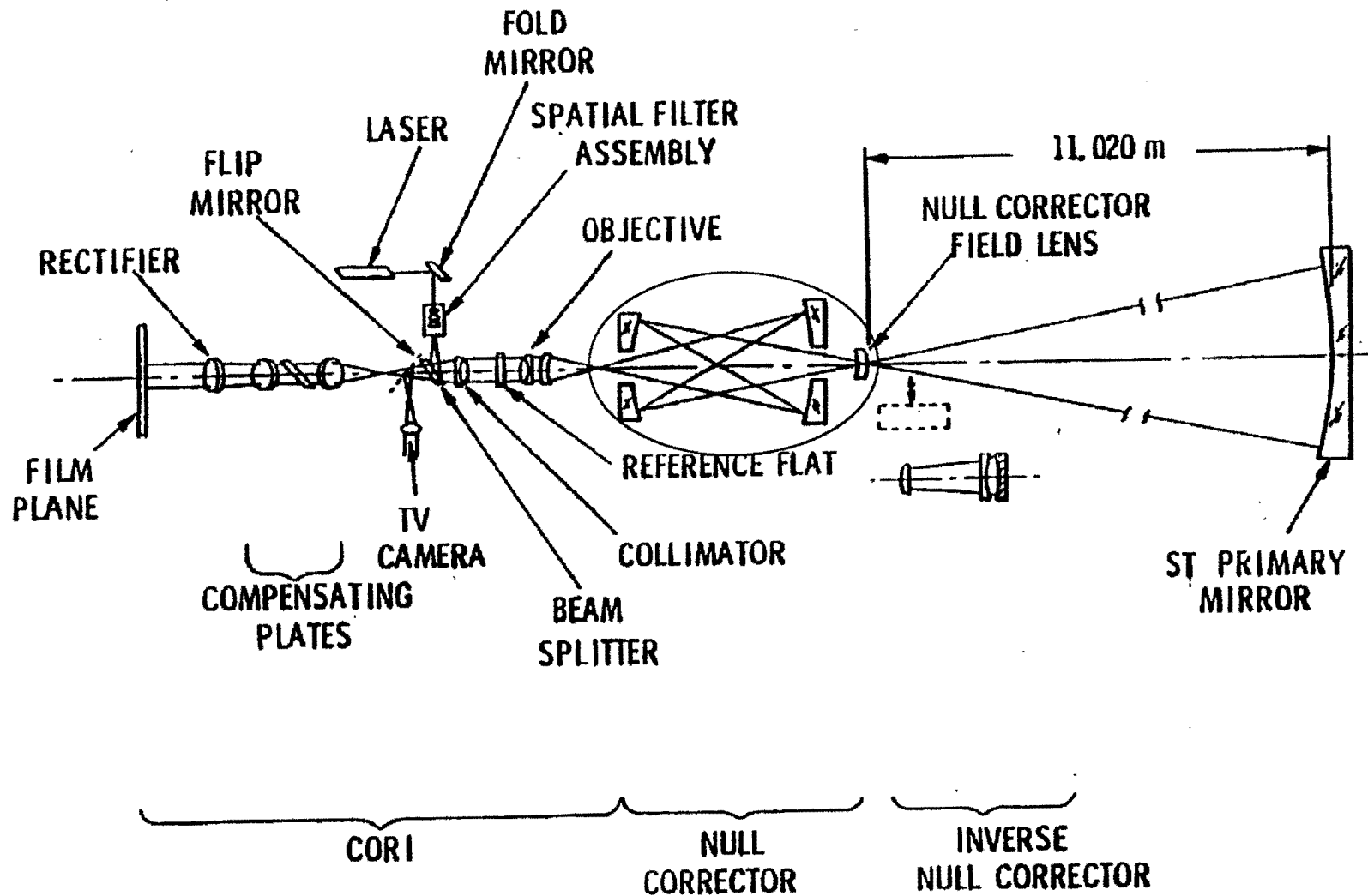
JPL WF/PC2 Team
Build camera and relay
optics to fix problem

(JRF, subcontractor)

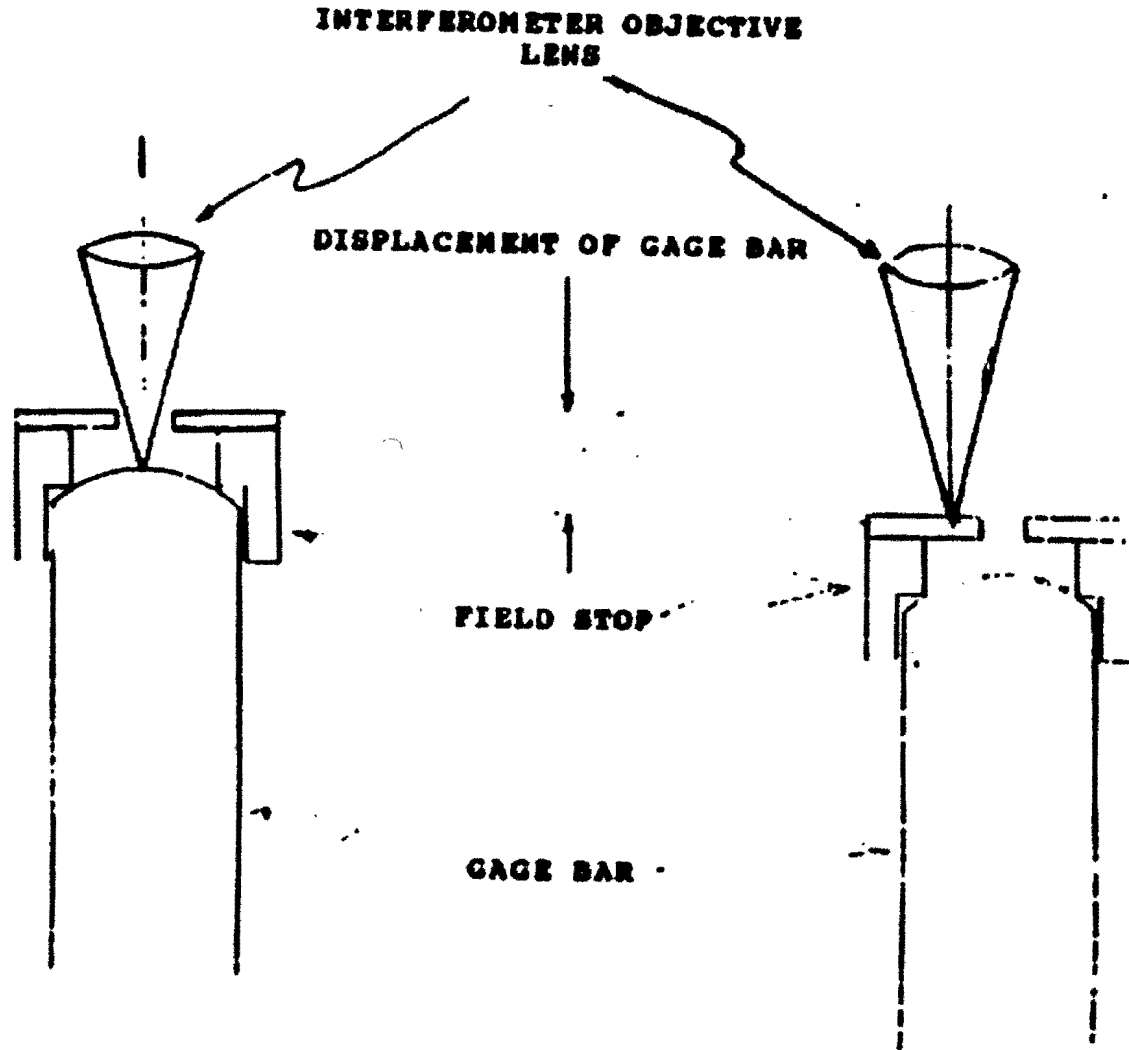
Space Telescope
Science Institute
Process imagery

Hughes Danbury
Optical System
Characterize problem,
align system

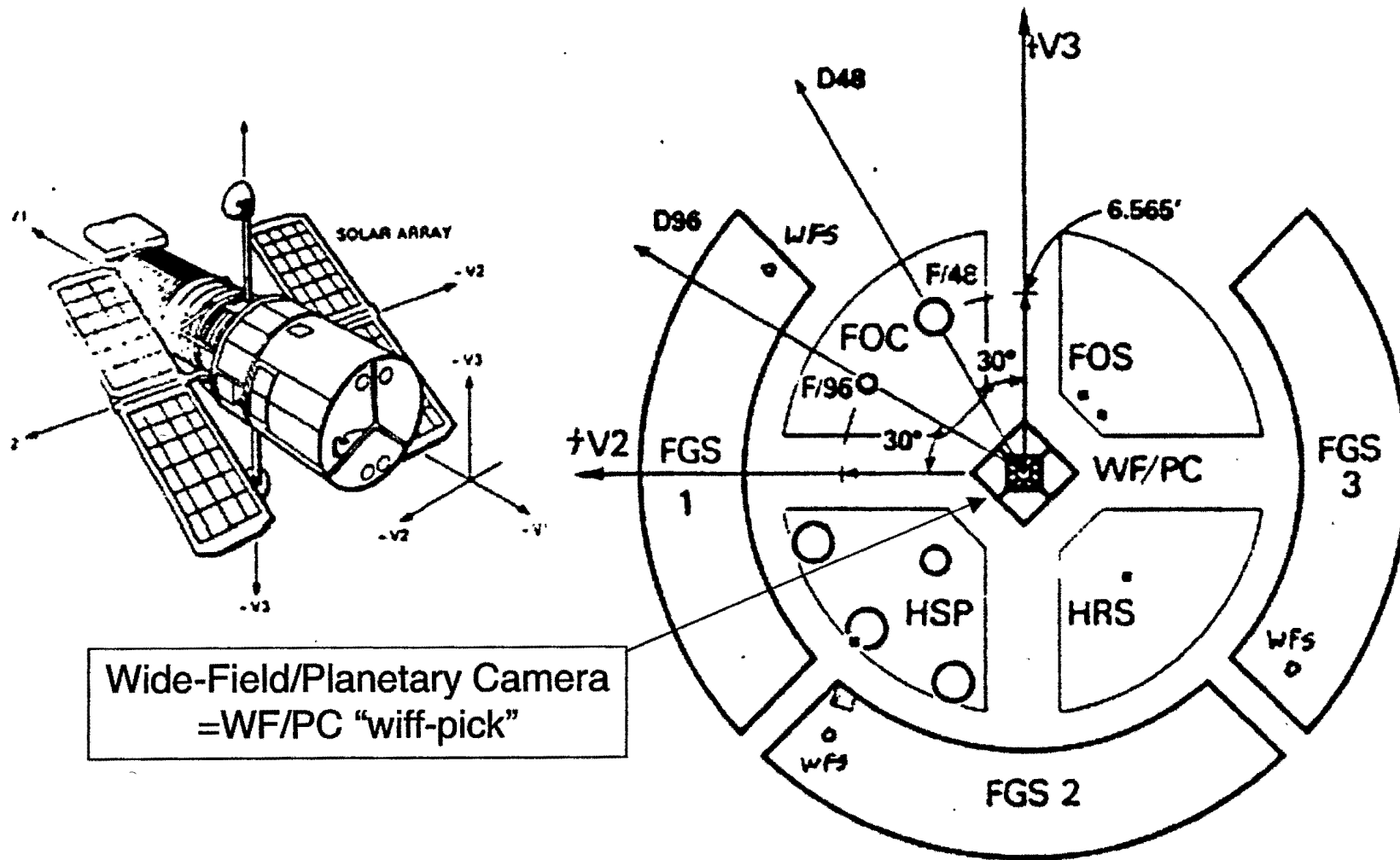
HST Ground & Polished According to Interferometer Measurements



1.3 mm Mistake in Null Corrector Spacing Causes 2 μm Mistake in Primary Mirror



HST Focal Plane

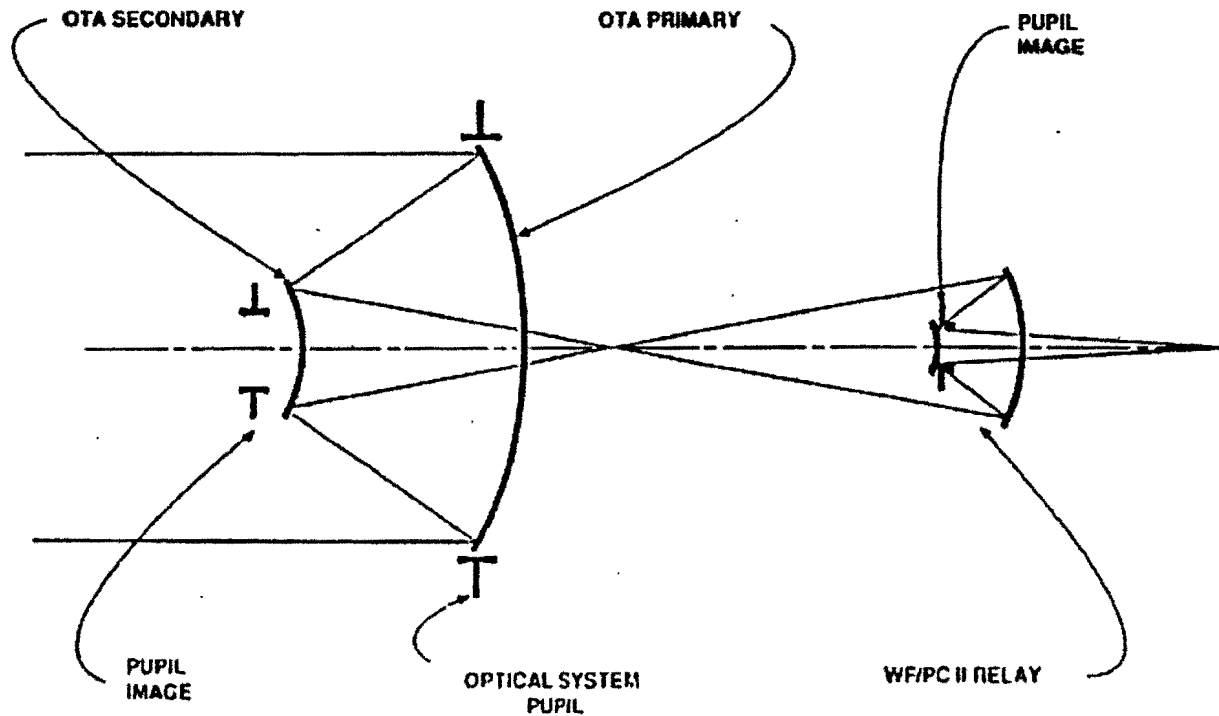


FRANK ESPINOZA

K. LESCHLY

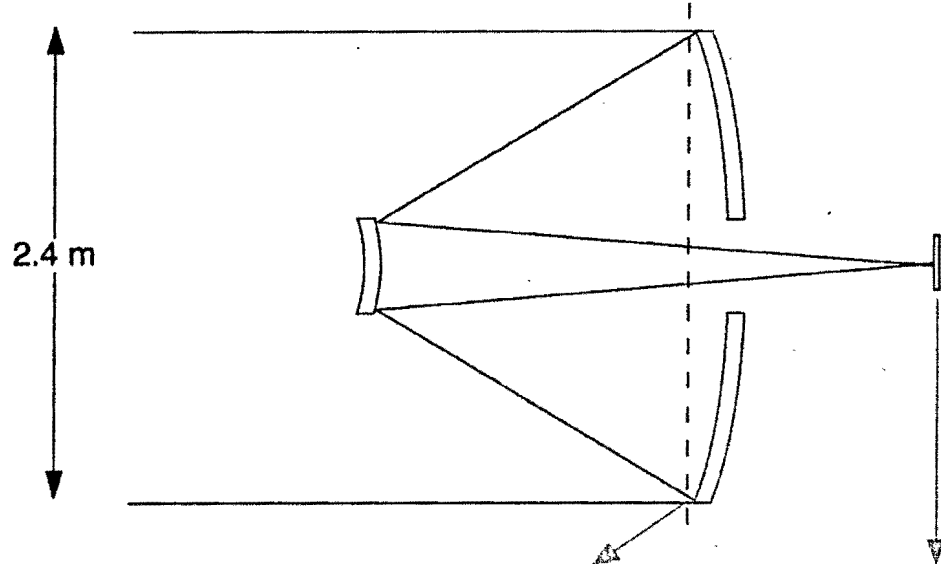
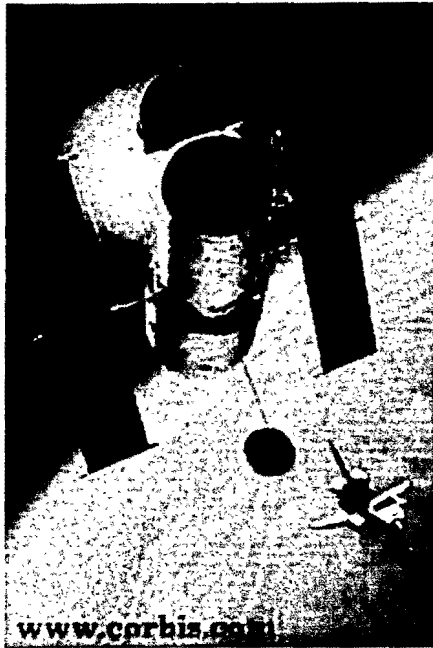


CORRECTION APPROACH

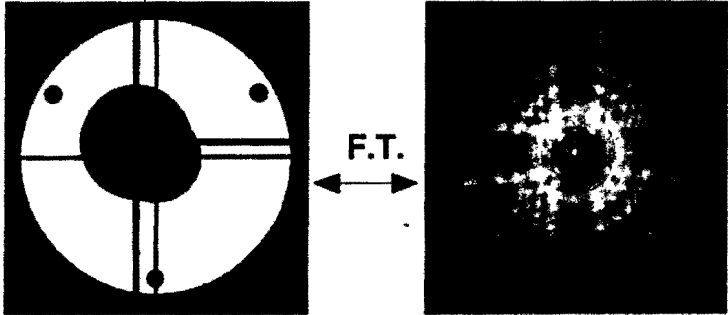


(Not to scale)

Determine HST Aberrations from PSF



Measurements & Constraints:
Pupil plane: known aperture shape
phase error fairly smooth function
Focal plane: measured PSF intensity



(Hubble Space Telescope)

Wavefronts in pupil plane and focal plane
are related by a Fourier Transform

Knowing aberrations precisely allows for:

- Design correction optics to fix the HST
 - WF/PC II
 - COSTAR
- Optimize alignment of secondary mirror of HST OTA
- Monitor telescope shrinkage (desorption) and focus
- Compute analytic point-spread functions for image deconvolution
 - Noise-free
 - Depends on λ , $\Delta\lambda$, camera, field position
 - Is highly space-variant for WF/PC
 - Eliminates requirement to measure numerous PSF's

In addition, reconstruction of pupil function allows determination of alignment between OTA and WF/PC

Focal plane field

Pupil plane field

$$\begin{aligned} \text{Fourier transform: } F(u, v) &= \int \int_{-\infty}^{\infty} f(x, y) e^{-i2\pi(ux + vy)} dx dy \\ &= |F(u, v)| e^{i\psi(u, v)} = \mathcal{F}[f(x, y)] \end{aligned}$$

Focal plane field magnitude
= sqrt(intensity)

Focal plane field phase

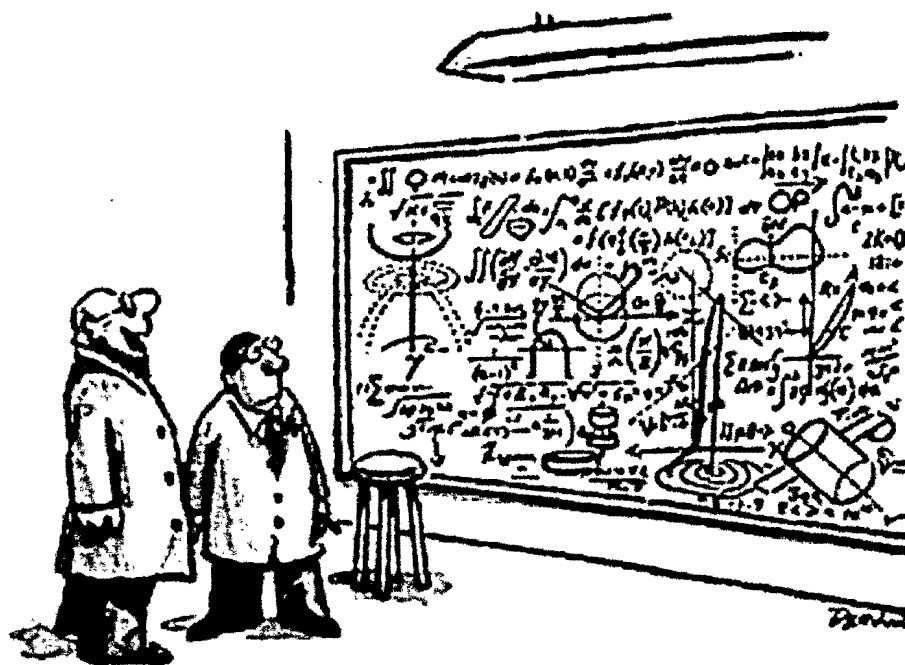
$$\text{Inverse transform: } f(x, y) = \int \int_{-\infty}^{\infty} F(u, v) e^{i2\pi(ux + vy)} dudv = \mathcal{F}^{-1}[F(u, v)]$$

Phase retrieval problem:

Given $|F(u, v)|$ and some constraints on $f(x, y)$,
Reconstruct $f(x, y)$, or equivalently retrieve $\psi(u, v)$

Equivalently, reconstruct field $f(x, y)$ in the pupil
— its phase is the phase error we wish to correct

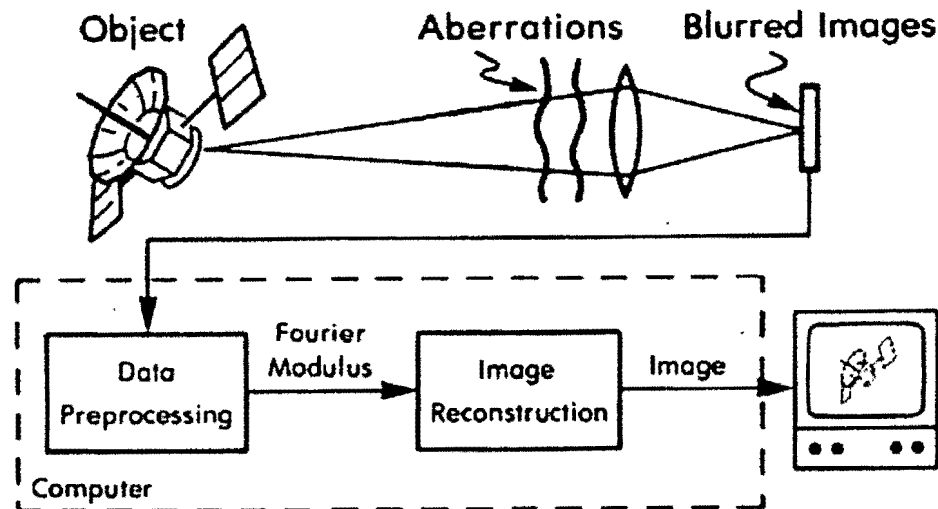
Is Phase Retrieval Possible?



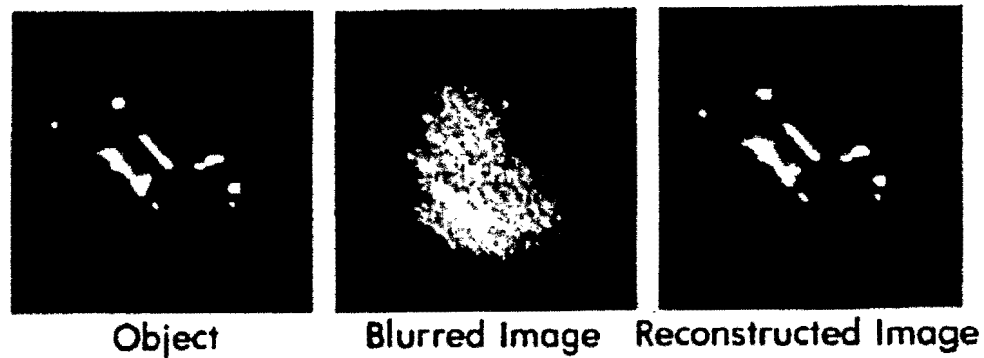
"Hey, no problem!"

Phase Retrieval for Image Reconstruction from Stellar Speckle Interferometry Data

IMAGING WITH PHASE ERRORS

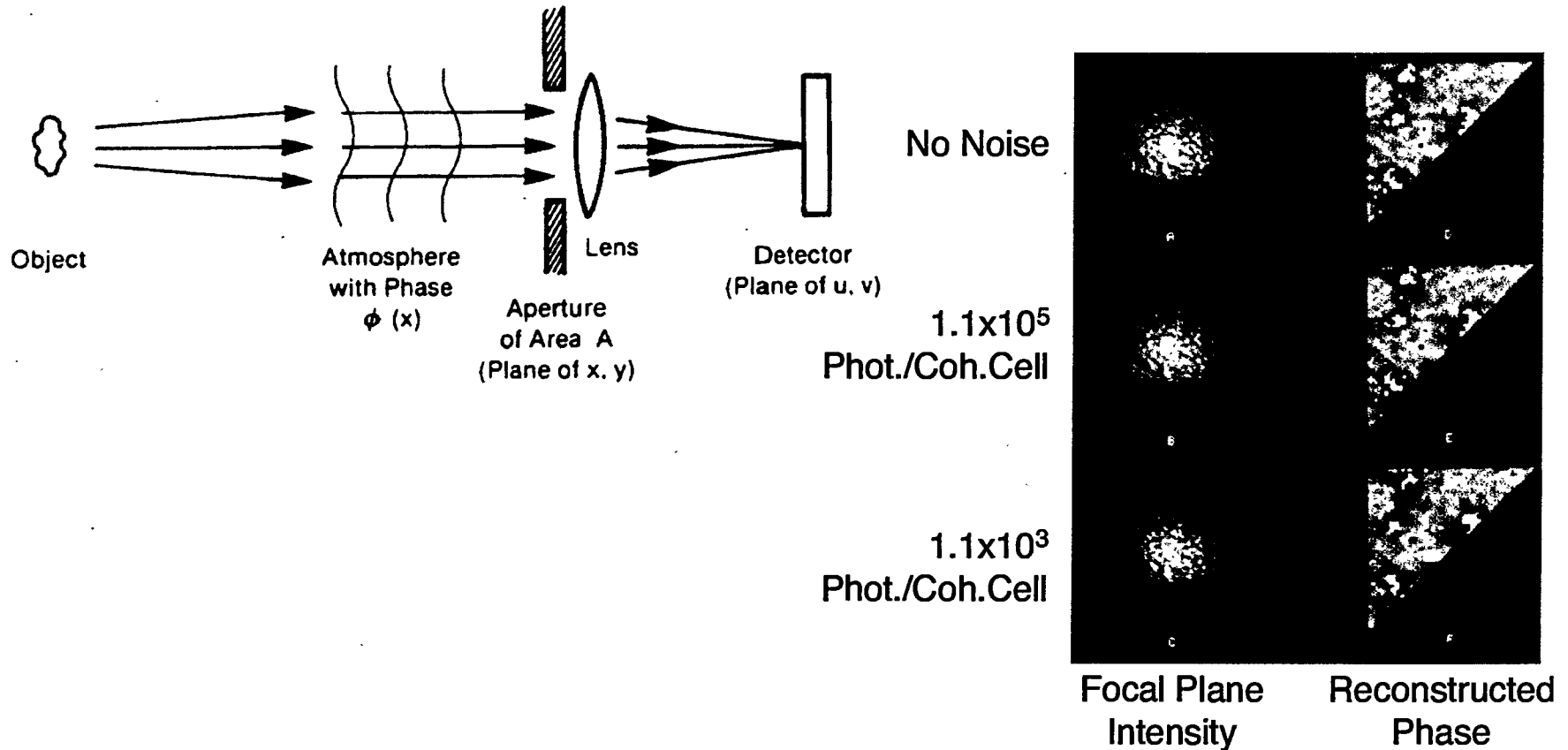


Example:



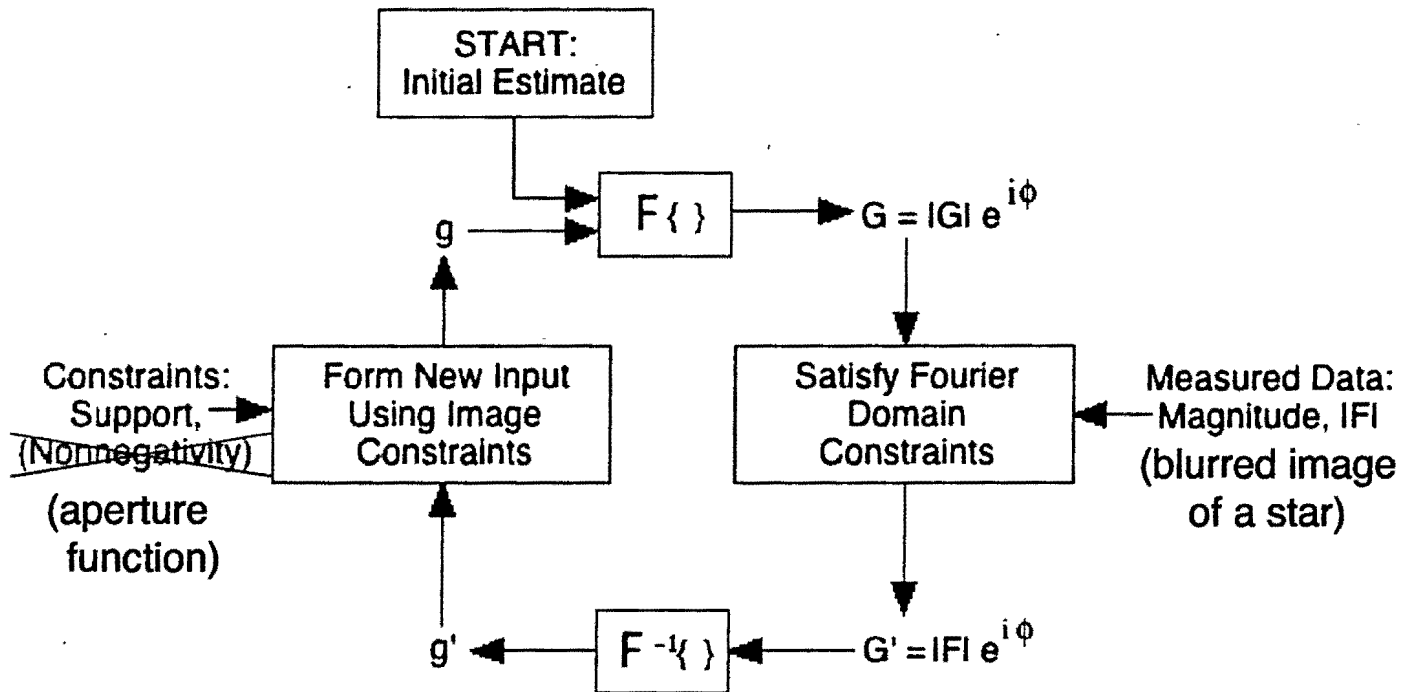
J.R. Fienup, "Phase Retrieval Algorithms: A Comparison," *Appl. Opt.* 21, 2758-2769 (1982).

Fourier Intensity Wavefront Sensor



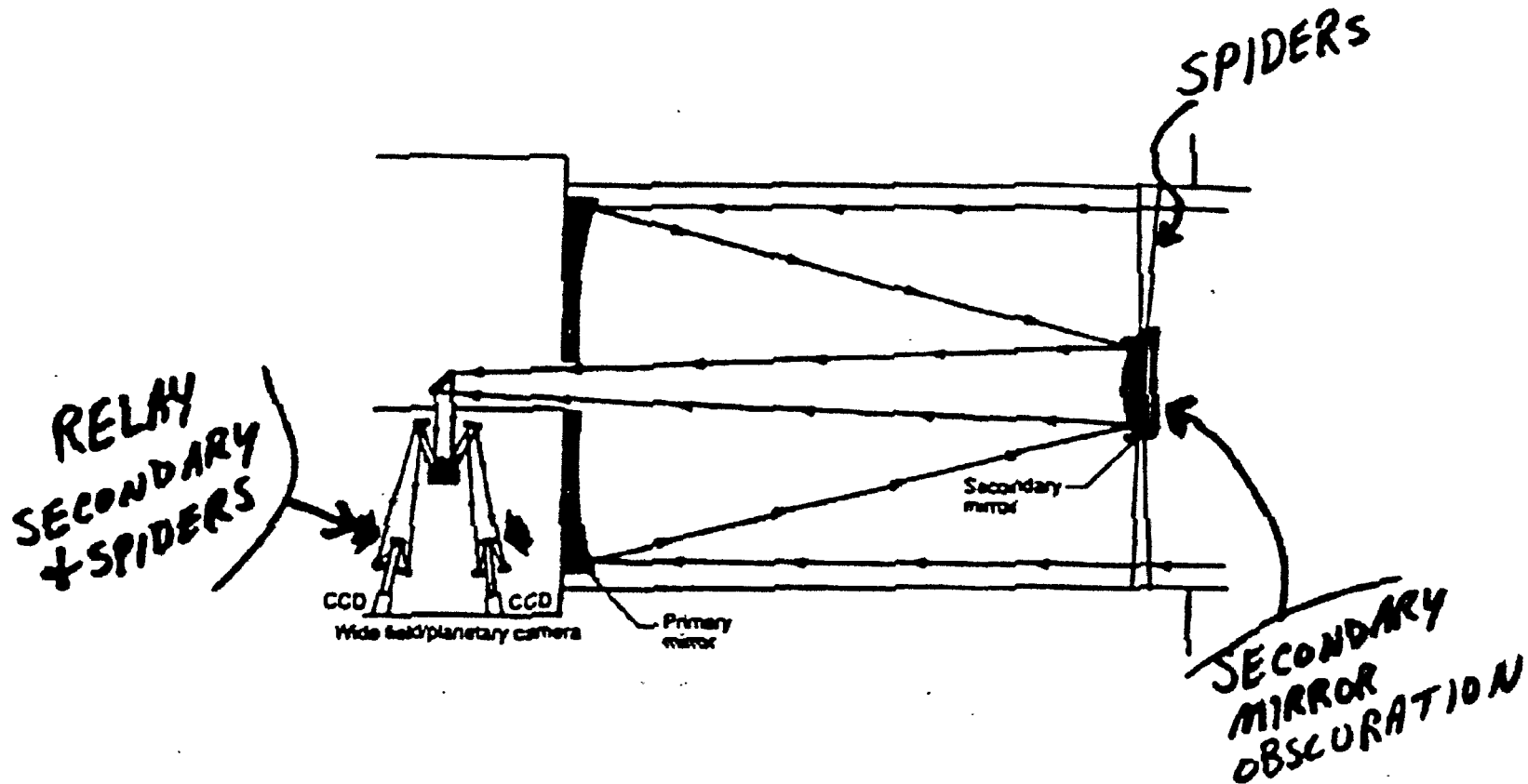
J.N. Cederquist, J.R. Fienup, C.C. Wackerman, S.R. Robinson and D. Kryskowski, "Wave-Front Phase Estimation from Fourier Intensity Measurements," J. Opt. Soc. Am. A 6, 1020-1026 (1989).

Iterative Transform Algorithm

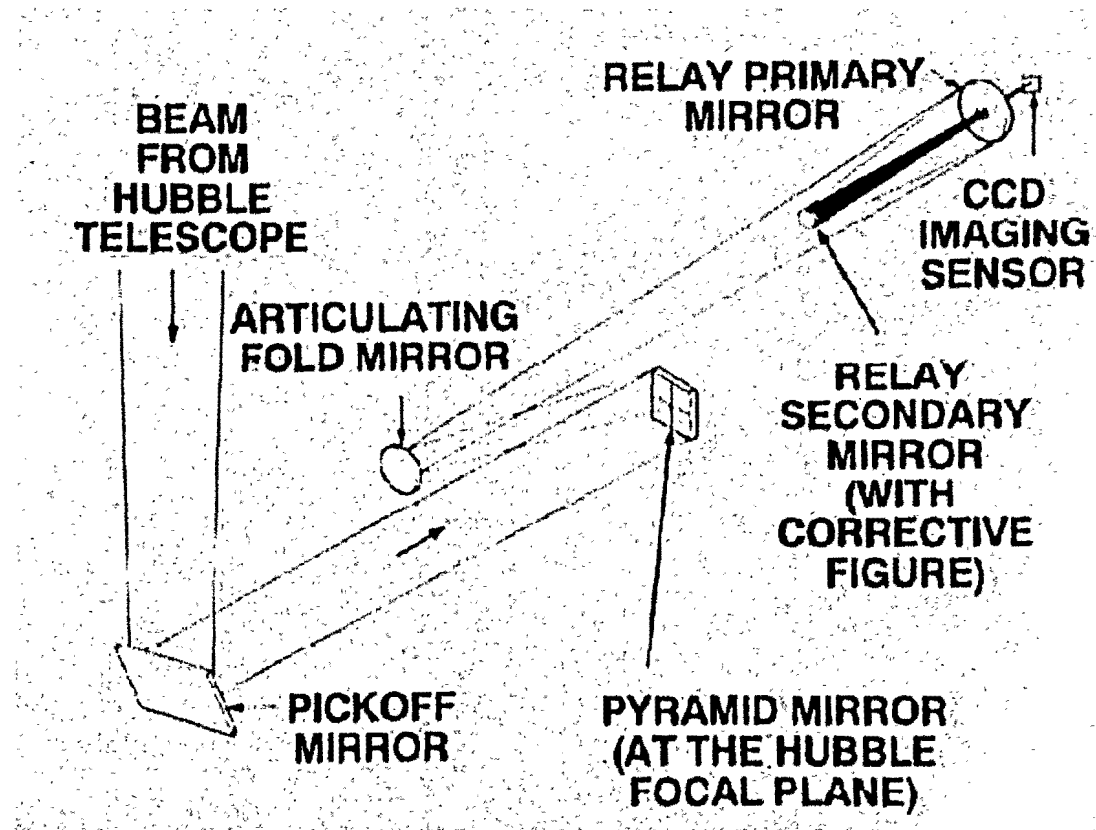


Enforcing magnitude constraints in both domains is the "Gerchberg-Saxton" algorithm

Sources of Obscurations in HST



WF/PC Camera Details



- Relay telescope secondary obscuration appears to translate vs. field angle

Minimize error metric by

- Cut & try [Jon Holtzman (Lowell Observatory)]
- Iterative transform algorithm (Gerchberg-Saxton/Misell/Fienup)
- Gradient search (steepest descent, conjugate gradient, . . .)
- Damped least squares (Newton-Raphson)
- Neural network [Todd Barrett & David Sandler (Thermo Electron)]
- Linear programming
- Prescription retrieval [David Redding (Draper Lab)]
- Phase diversity
- etc. (intensity transport, tracking zero sheets, simulated annealing, ...)

- Other groups doing phase retrieval
 - Rick Lyon *et al.* Hughes Danbury Optical Systems
 - Chris Burrows (Space Telescope Science Institute)
 - Mike Shao *et al.* (JPL)
 - Francois Roddier (U. Hawaii), . . .

- Model optical system
 - Known parameters (constraints)
 - Unknown parameters (to retrieve)
- Compute model of data
- Compare model of data with actual measured data
 - Compute error metric
- Minimize error metric over space of unknown parameters
 - Using nonlinear optimization algorithms

Detector plane:

Computed

Measured

$$\rightarrow E_1^2 = \sum_u W(u) [|G(u)| - |F(u)|]^2$$

$$E_2^2 = \sum_u W(u) [|G(u)|^2 - |F(u)|^2]^2$$

Maximum likelihood
for additive Gaussian noise

$$E_3^2 = \sum_u W(u) \{ |G(u)| - |F(u)| - |G(u)| \ln [|F(u)| / |G(u)|] \}^2$$

$$L = - \sum_u W(u) |G(u)|^2 + \sum_u W(u) |F(u)|^2 \ln [|G(u)|^2]$$

Maximum likelihood
for Poisson noise

Aperture plane:

— Treating detector-plane phase as optimization parameters

$$E_{ap}^2 = \sum_x [|g(x)| - |f(x)|]^2$$

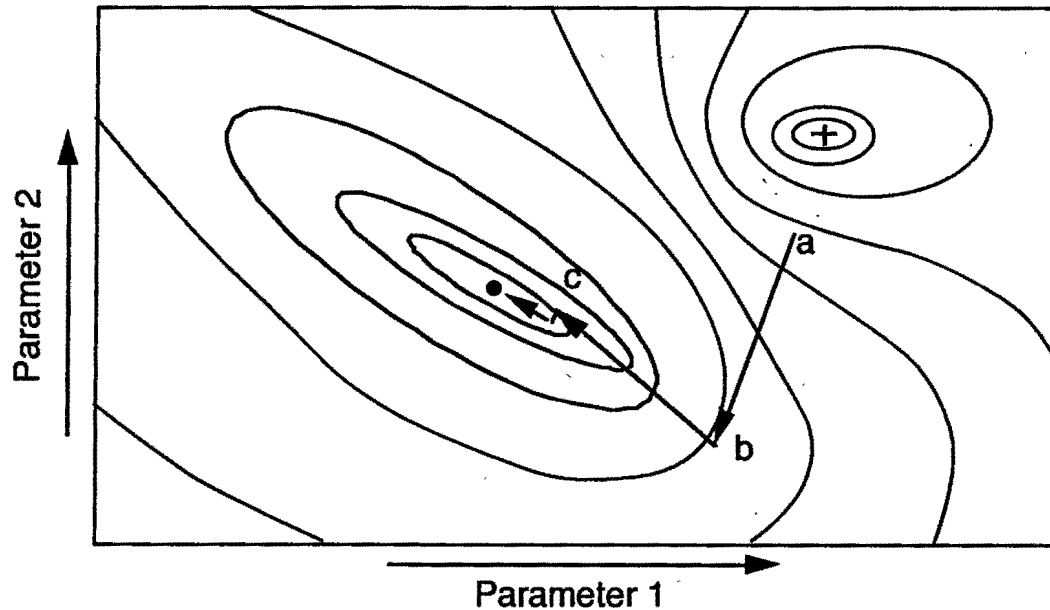
etc.

Computed

Known Pupil

Minimize Error Metric, e.g.: $E = \sum_u W(u)[|G(u)| - |F(u)|]^2$

Contour Plot of Error Metric



Repeat three steps:

1. Compute gradient:

$$\frac{\partial E}{\partial p_1}, \frac{\partial E}{\partial p_2}, \dots$$

2. Compute direction of search

3. Perform line search

Gradient methods:

(Steepest Descent)

Conjugate Gradient

BFGS/Quasi-Newton

...

Analytic Gradients of $E = \sum_u W(u) [|G(u)| - |F(u)|]^2$

Pupil:

$$g(x) = m_o(x) e^{i\theta(x)}$$

$$g^W(x) = P^\dagger [G^W(u)]$$

Detector plane:

$$G(u) = P[g(x)]$$

$$G^W(u) = W(u) \left[|F(u)| \frac{G(u)}{|G(u)|} - G(u) \right]$$

Derivative w.r.t. general parameter: $\frac{\partial E}{\partial \rho} = -2 \operatorname{Re} \left[\sum_x \frac{\partial g(x)}{\partial \rho} g^{W*}(x) \right]$

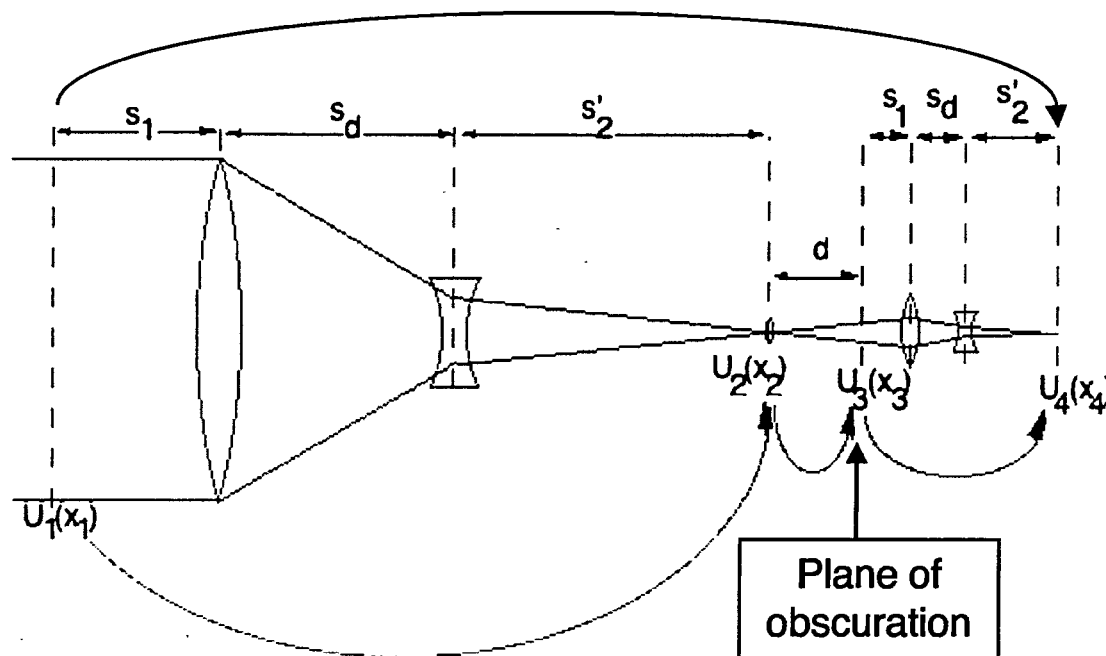
For point-by-point phase map, $\theta(x)$, $\frac{\partial E}{\partial \theta(x)} = 2 \operatorname{Im} \{ g(x) g^{W*}(x) \}$

For Zernike polynomial coefficients, $\frac{\partial E}{\partial a_j} = 2 \operatorname{Im} \left\{ \sum_x g(x) g^{W*}(x) Z_j(x) \right\}$
 where $\theta(x) = \sum_{j=1}^J a_j Z_j(x)$

Propagator $P[\cdot]$ can be single FFT
 or multiple-plane Fresnel transforms
 with phase factors and obscurations

Analytic gradients very fast
 compared with finite differences

- Simple Fourier propagation
 - All obscurations, phase errors in same plane
 - Phase errors in two mirrors, wavefront translates with field angle

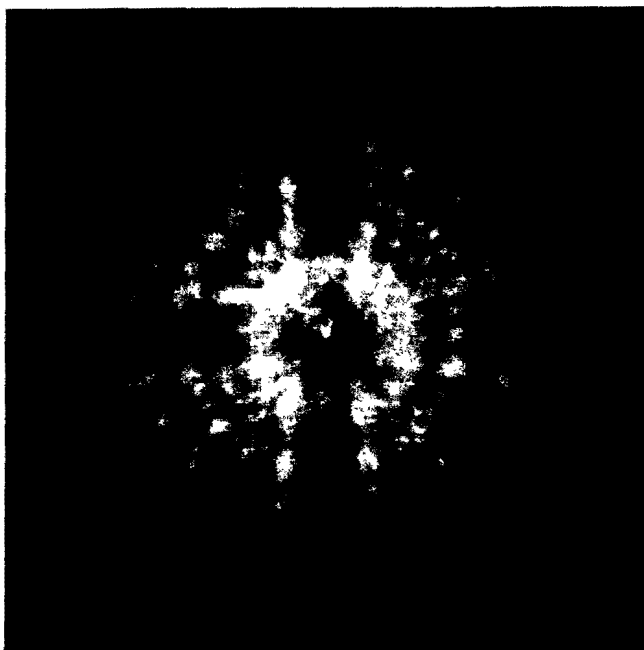


Thin lens model
of HST + PC

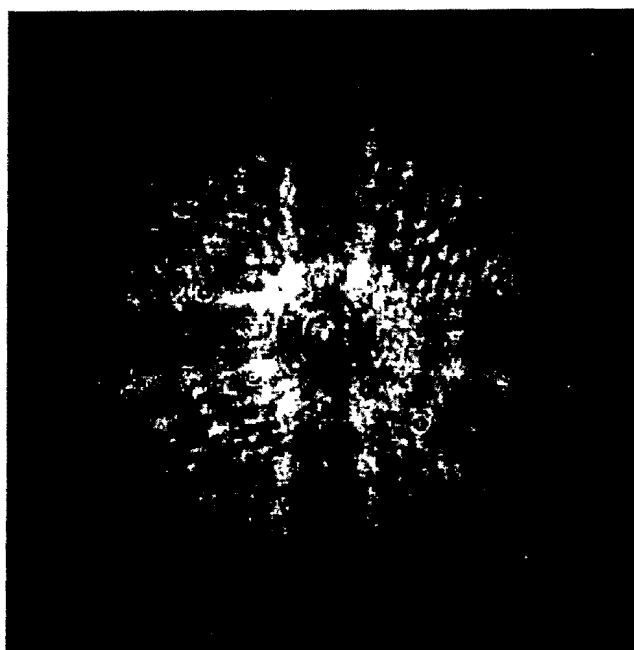
- Fresnel propagation, using multiple planes of diffraction
 - Obscurations planes, phase error planes

- Multi-plane propagation including vignetting or multiple aberration planes
- Jitter in telescope pointing during exposure time
- Exclude bad pixels from error metric (dust/saturation/cosmic rays)
- Finite spectral bandwidth
- Shifted WF/PC obscurations vs. field position
- Correct plate scale (depends on field position)
- CCD pixel integration, sampling (undersampling/aliasing)
- Include model of noise (photon, readout)
- Higher-order Zernike's and micro-roughness
- Effect of aberrations in OTA secondary, in WF/PC cameras
- Design aberrations versus field position
- Possibility of non-point-like star

Dust Artifacts and Glitches in WF/PC Images

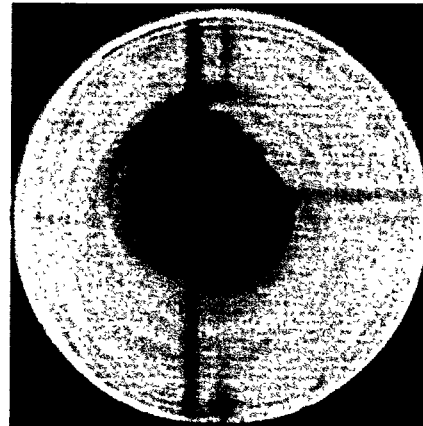


Raw image (point source)

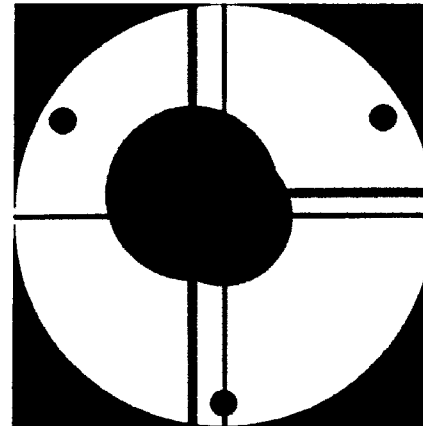


Sharpened image

- Pupil (support constraint) was known imperfectly
 - Phase was relatively smooth and dominated by low-order Zernike's
 - Use boot-strapping approach
1. With initial guess for pupil, fit Zernike polynomial coefficients
 2. With initial guess for Zernike polynomials, estimate pupil by ITA



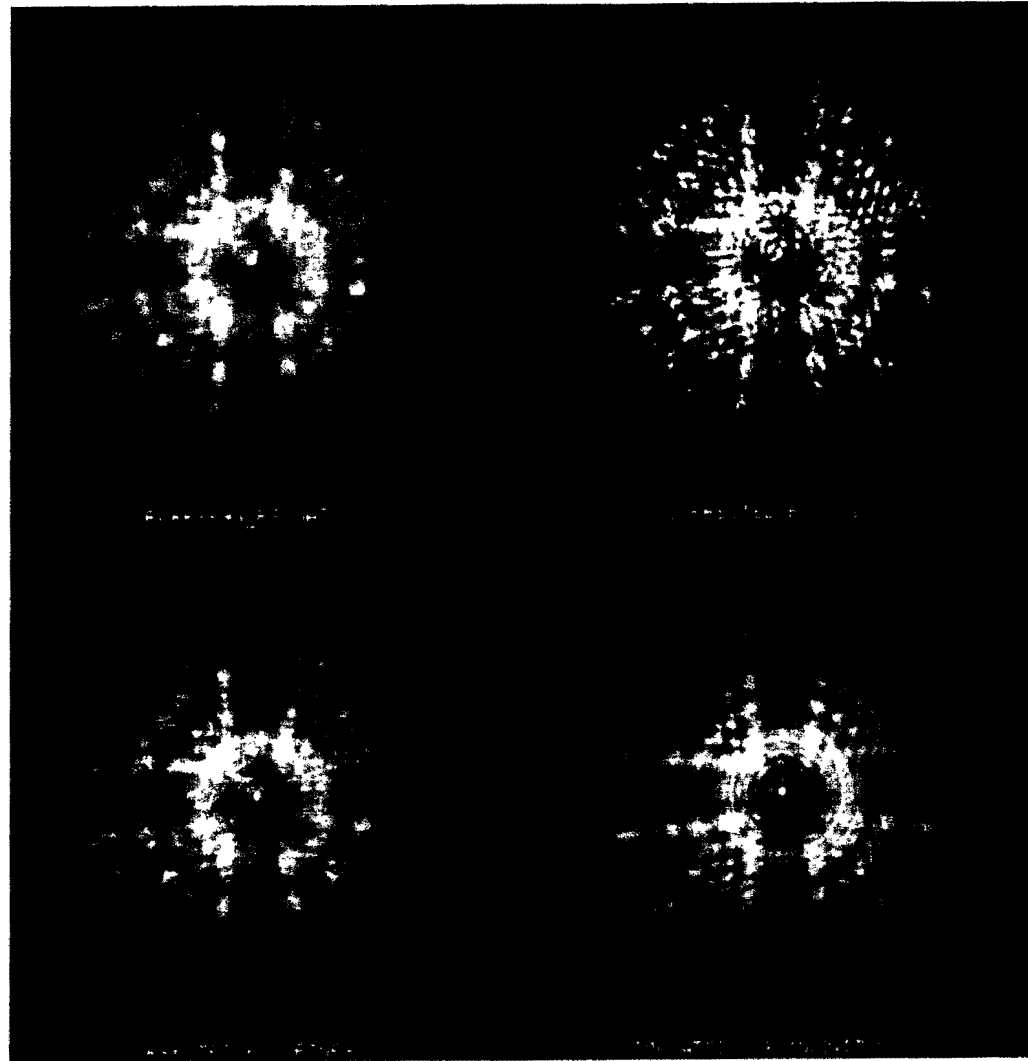
Pupil Reconstructed
by ITA



Inferred Model of Pupil

3. Redo steps 1 and 2 until convergence (2 iterations)

Comparison of Actual and Simulated HST Image of a Point Star



ERIM Phase Retrieval Results

Greater Accuracy --> Larger Z11 Values

- Results -- PC6 F889N_P2 data ($\Delta z = -260$):

Zernike Coefficients (microns rms of wavefront error):

Zernike Coefficient	Single	Multi(11)	Multi(22)	New Param. Multi(11)
4	-2.212	-2.227	-2.223	-2.303
5	-0.018	-0.003	0.006	-0.003
6	-0.025	0.025	0.026	0.031
7	0.004	0.001	0.005	-0.001
8	0.017	0.010	0.009	0.013
9	-0.022	-0.020	-0.009	-0.021
10	0.002	0.008	0.010	0.005
11	-0.280	-0.292	-0.295	-0.300
12	0.008			
16	-0.009		-0.004	
20	0.006			
22	0.005	0.006	0.007	0.008
conic κ =	-1.0144	-1.0151	-1.0152	-1.01545
rms err =	0.1583	0.1352	0.1353	

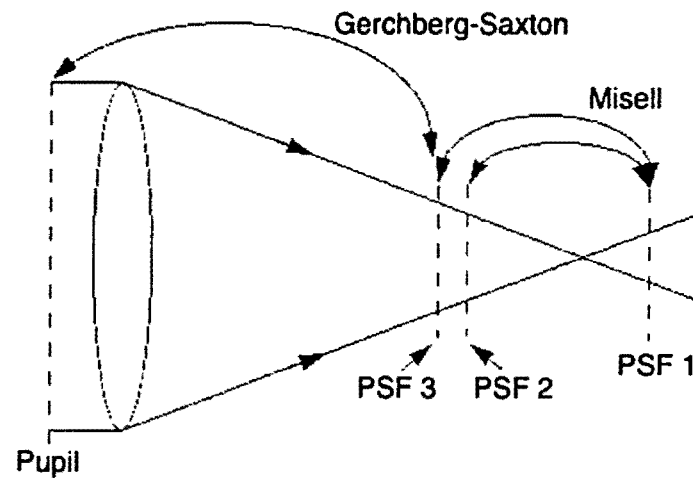
New parameters: Plate scale = 0.0442 arcsec/pixel, bq = -0.000059

John Holtzman (Lowell Observatory)

“Cut and Try” = compare images with various computed spherical

Francoise & Claude Roddier

Miselle algorithm



Aden B. Meinel, Marjorie P. Meinel, and Daniel H. Schulte, "Determination of the Hubble Space Telescope effective conic-constant error from direct image measurements," *Appl. Opt.* 32, 1715-1719 (1993).



Fig. 2. Typical PC-6 image showing the points defining the center of the pad diffraction spot and the periphery of the image.

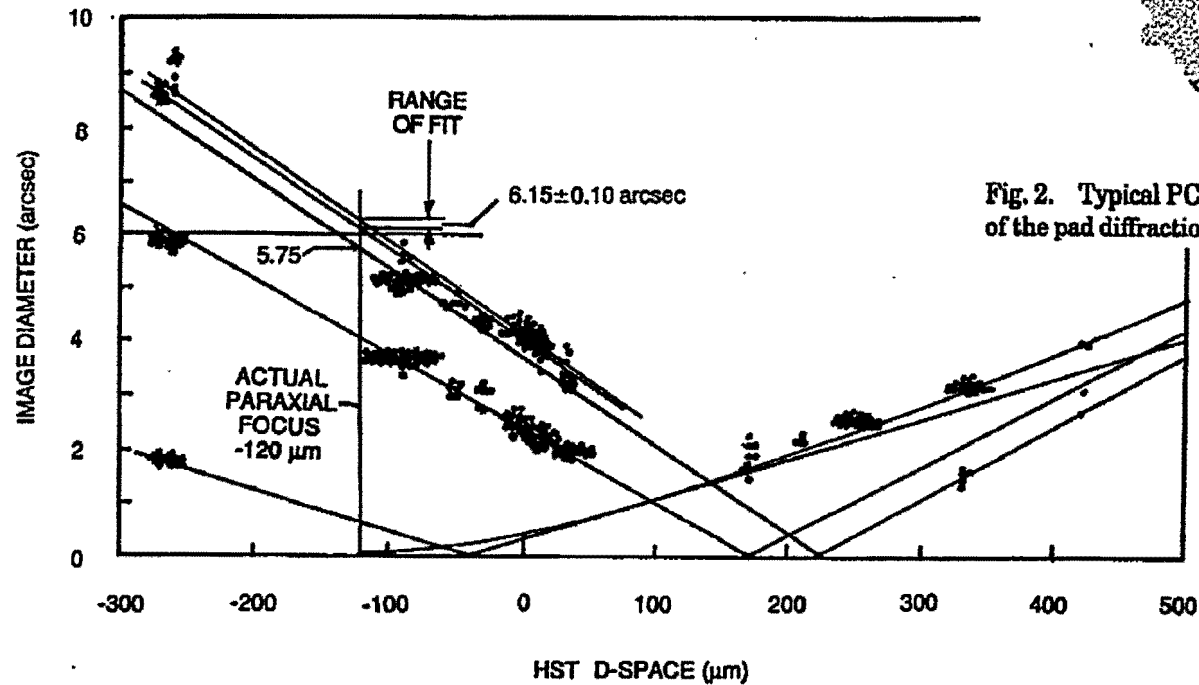
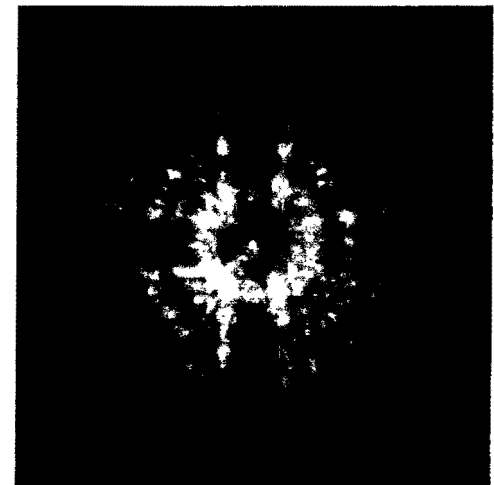
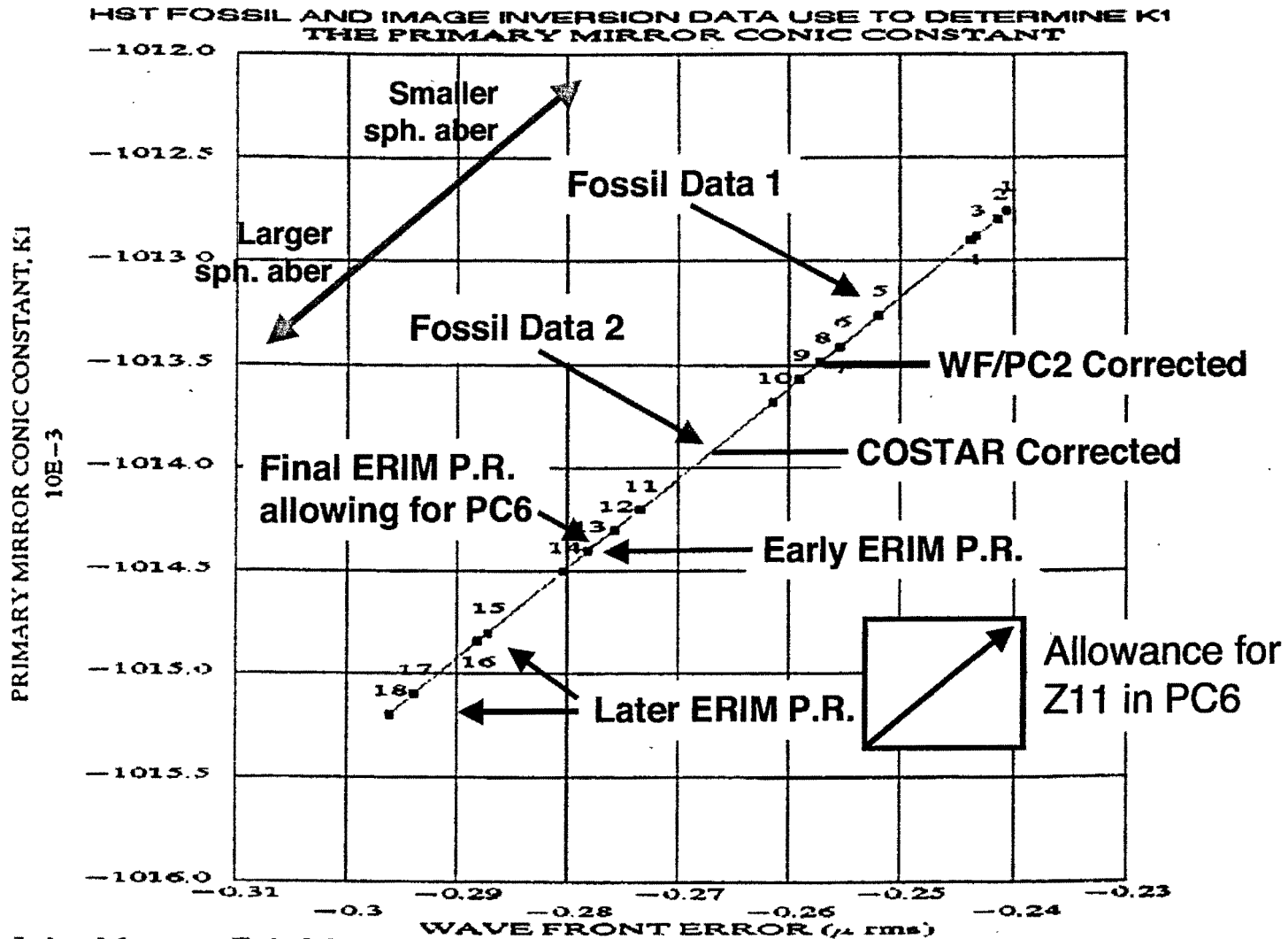


Fig. 5. Best fit of measured points to the Schulte lines defines the paraxial focus as being at $-120 \mu\text{m}$ and the rim image diameter as being $6.15 \pm 0.1 \text{ arcsec}$. This leads to an apparent conic constant of -1.01429 ± 0.0002 .



Discrepancy with Phase Retrieval Caused NASA to Look for Additional Errors



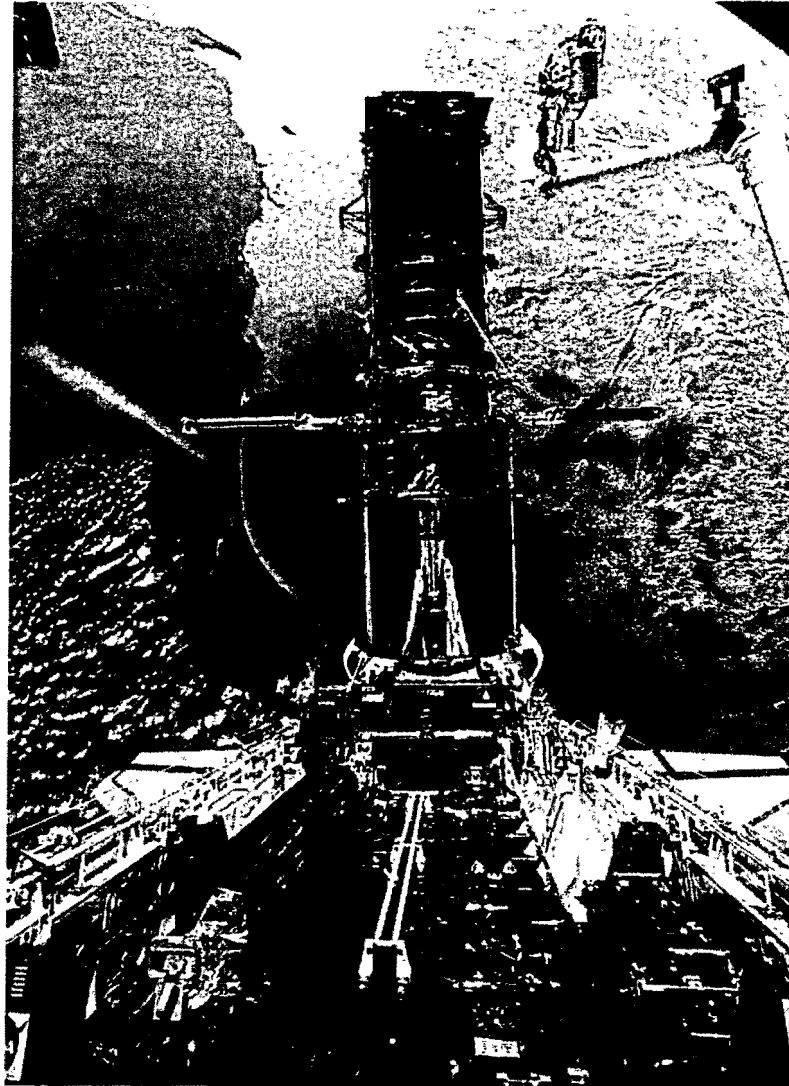
John Mangus Feb 26, 1991

Sources of Estimates of Spherical Aberration

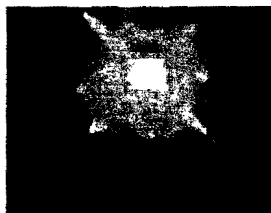
DATA SOURCE	CONIC CONSTANT	ERROR BARS	WFE (μ rms)	ERROR BARS (μ rms)
				26-Feb-91
1 WETHERELL: RNC, note 1	-1.01276 \pm		-0.2405 \pm	
2 MANGUS: INC, note 2	-1.01280 \pm	0.0008	-0.2415 \pm	0.0183
3 FUREY: RvNC, note 3	-1.01288		-0.2433	
4 FUREY: RNC, note 1	-1.01290 \pm	0.0002	-0.2437 \pm	0.0046
5 MANGUS : RvNC, note 4	-1.01326 \pm	0.0008	-0.2520 \pm	0.0183
6 MIENELS': PAD LOCATION	-1.01341 \pm		-0.2554 \pm	
7 MIENELS' : RIM IMAGE	-1.01342 \pm		-0.2556 \pm	
8 FUREY : RNC, note 5	-1.01349 \pm	0.0006	-0.2571 \pm	0.0137
9 LYONS : HDOS-FOC, HARP I	-1.01357 \pm		-0.2590 \pm	0.0005
10 BURROWS: Sci-FOC, HARP I	-1.01368 \pm	0.0008	-0.2615 \pm	0.0183
11 FABER/HOLTZMANN : WF/PC-PC	-1.01420 \pm		-0.2734 \pm	0.0000
12 LYONS : HDOS-PC, HARP I	-1.01430 \pm	0.0005	-0.2757 \pm	0.0114
13 LYONS: HDOS-WF	-1.01440 \pm	0.0009	-0.2780 \pm	0.0205
14 RODIER : PC, HARP I	-1.01450 \pm		-0.2802 \pm	0.0000
15 BURROWS : HST Sci Inst-PC,HARP I	-1.01480 \pm	0.0003	-0.2871 \pm	0.0068
16 VAUGHN : PAD LOCATION	-1.01484 \pm	0.0003	-0.2881 \pm	0.0068
17 FIENUP : ERIM - PC, HARP I	-1.01510 \pm	0.0007	-0.2939 \pm	0.0160
18 SHAO : JPL-PC, HARP I	-1.01520 \pm		-0.2962 \pm	0.0000

- e 1; assumes M2 to FL, M1 to M2 and CORI to M1 errors are real
- e 2; assumes as built errors had correct spacing to correct
for element fab error
- e 3; assumes reticle in and EPI to NL distance adjusted by +.68 mm
- e 4; assumes earliest as built data given in August 1990, Allen Comm.
- e 5; assumes only FLPE as real , other spacing measurements as

Hubble Fixed



Greatly Improved Imagery



Small residual blurring
noticeable only for
bright point sources



Gaseous Pillars · M16

HST · WFPC2

PRC95-44a · ST ScI OPO · November 2, 1995
J. Hester and P. Scowen (AZ State Univ.), NASA

Phase-retrieval analysis of pre- and post-repair Hubble Space Telescope images

John E. Krist and Christopher J. Burrows

Phase-retrieval measurements of point-spread functions from the pre- and post-repair Hubble Space Telescope are presented. The primary goal was to determine the aberrations present in the second wide-field and planetary camera (WFPC2) to align and validate its corrective optics. With both parametric model-fitting techniques and iterative (Gerchberg-Saxton) methods, accurate measurements have been obtained of the WFPC2 and Hubble Space Telescope optics, including improved maps of the zonal errors in the mirrors. Additional phase-retrieval results were obtained for the aberrated, prerepair cameras and the corrected faint-object camera. The information has been used to improve models produced by point-spread-function simulation programs. On the basis of the measurements a conic constant for the primary mirror of $\kappa = -1.0144$ has been derived.

WF/PC2 corrected to
 $\kappa = -1.0135$ ($Z_{11} = -0.254 \mu\text{m}$)
COSTAR corrected to
 $\kappa = -1.0139$ ($Z_{11} = -0.263 \mu\text{m}$)
Fienup 1991 (after $-0.013 \mu\text{m}$ PC)
 $\kappa = -1.0144$ ($Z_{11} = -0.276 \mu\text{m}$)
Krist & Burrows 1995 agrees

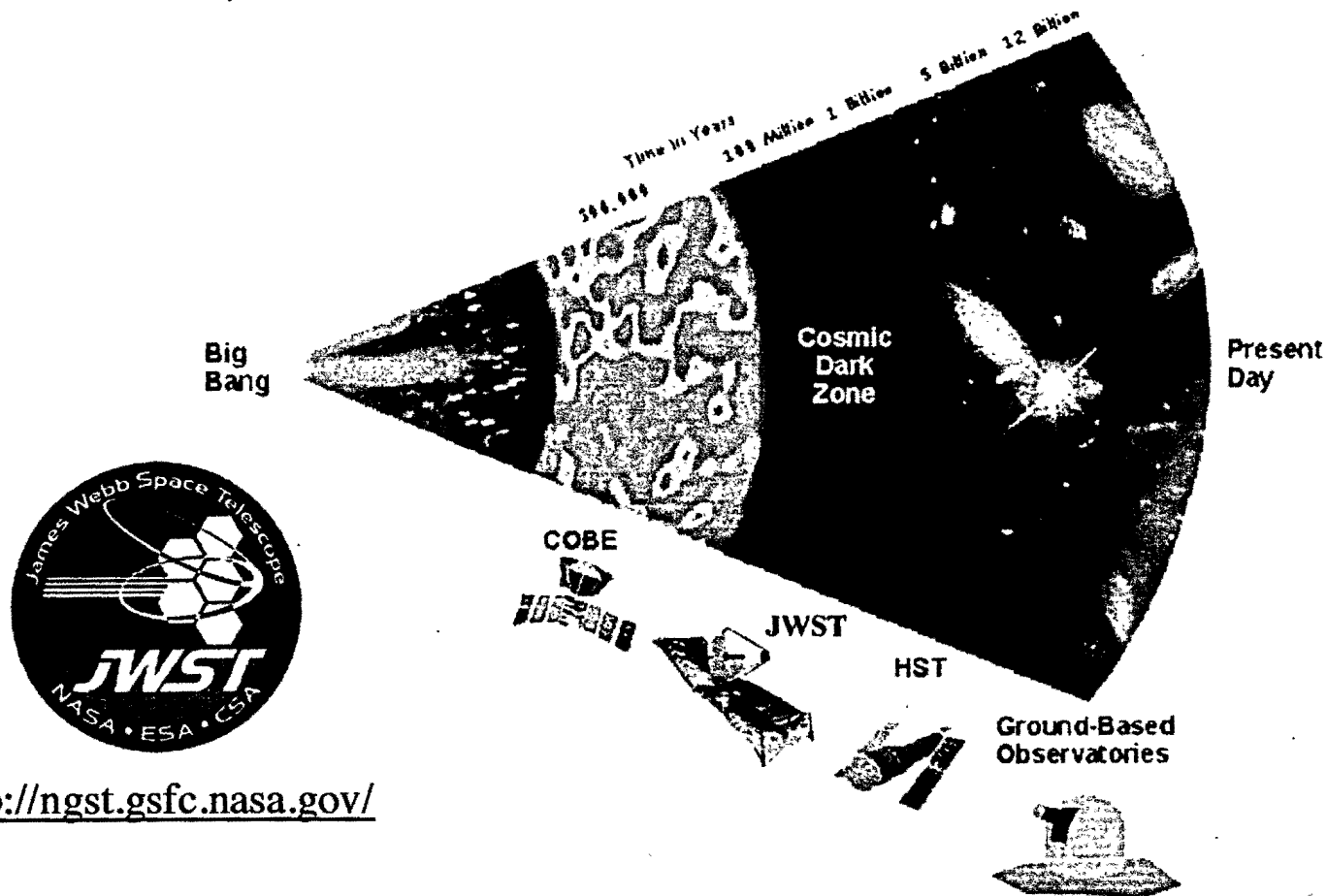
1 August 1995 / Vol. 34, No. 22 / APPLIED OPTICS 4951

Our results for WFPC2 indicated that the compromise conic constant derived by the HIORP underestimated the spherical aberration by a small but measurable amount.

"Hubble Space Telescope Characterized by using Phase-Retrieval Algorithms, J.R. Fienup, J.C. Marron, T.J. Schulz, and J.H. Seldin, *Appl. Opt.* **32**, 1747-1767 (1993).

James Webb Space Telescope

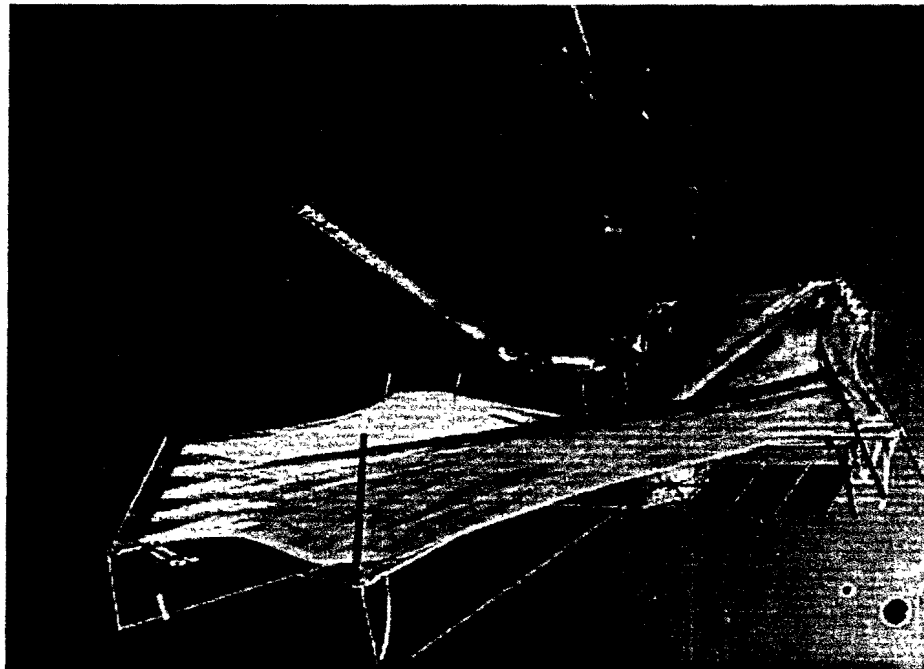
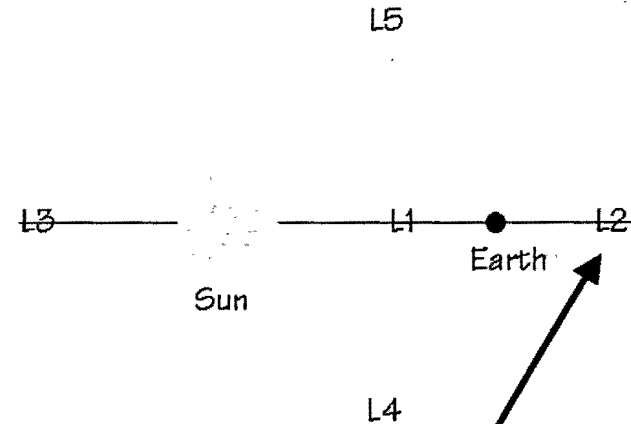
(Next Generation Space Telescope)

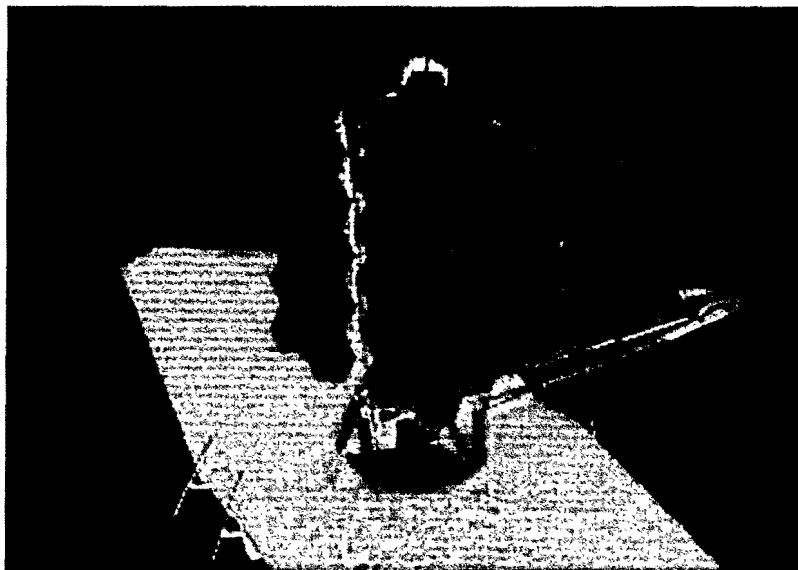
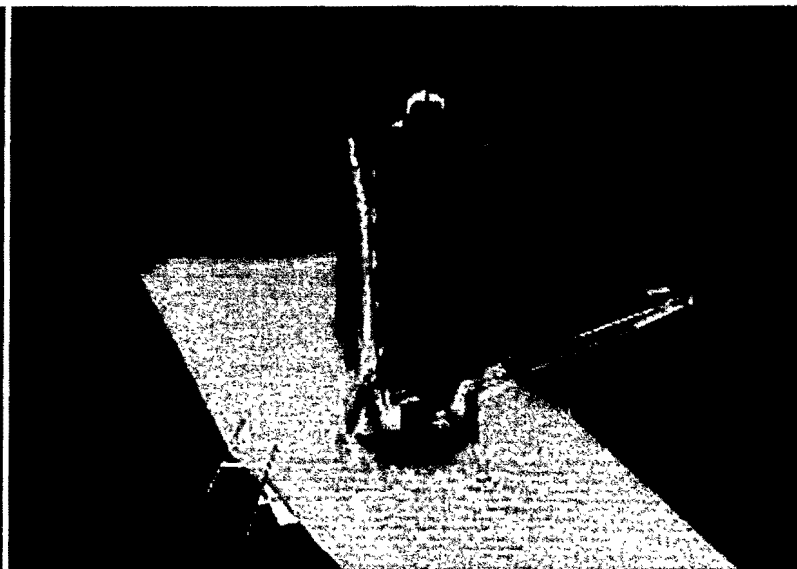
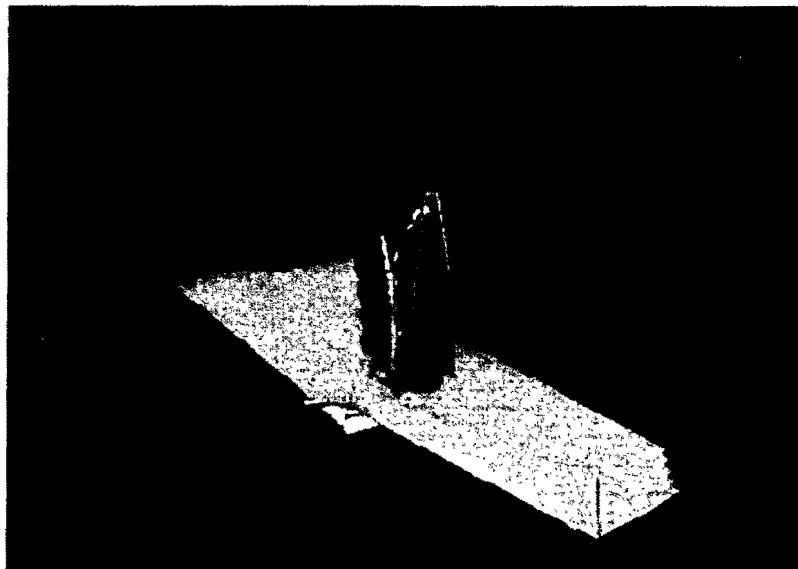


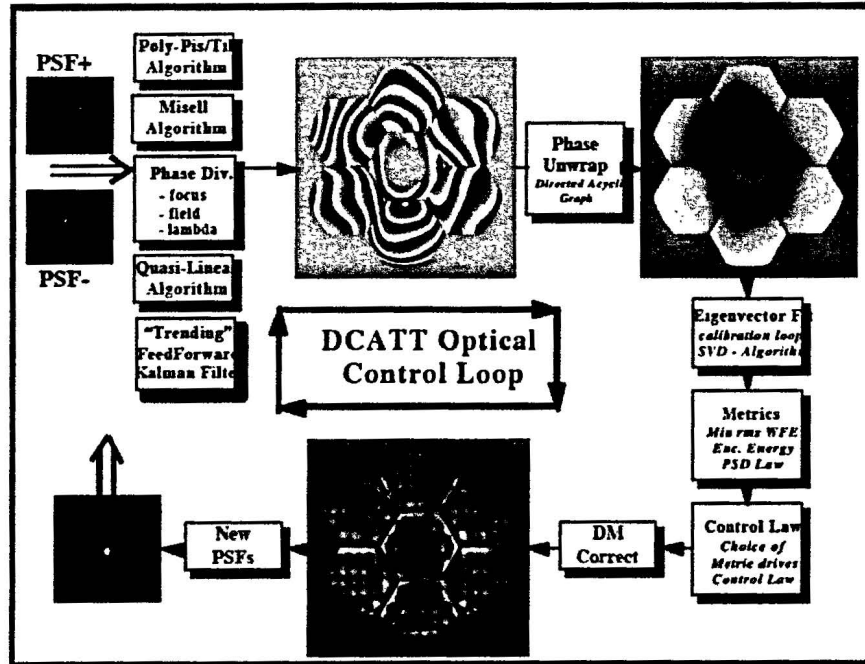
<http://ngst.gsfc.nasa.gov/>

See farther back towards the beginnings of the universe
Light is red-shifted into infrared

- See red-shifted light from early universe
 - 0.6 μm to 28 μm
 - L2 orbit for passive cooling, avoiding light from sun and earth
 - 6.6 m diameter primary mirror
 - Deployable, segmented optics
 - Phase retrieval to align segments







R. Lyon et al., (GSFC)

NASA has chosen phase retrieval as the fine phasing approach for JWST.

Wavefront Estimate Using $\pm 2 \lambda$ Defocus Imagery (1% Passband)

Wavefront Estimate Using $\pm 8 \lambda$ Defocus Imagery (1% Passband)

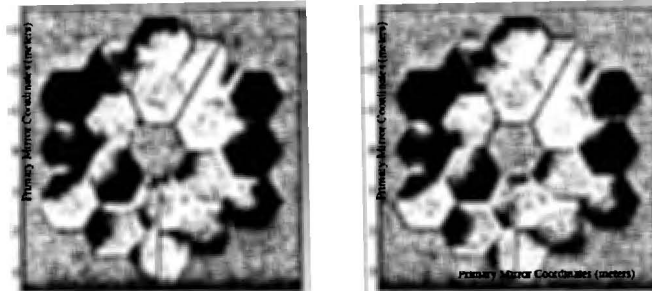


Figure 3: Estimates of the JWST OPD from the ± 2 wave defocus PSF pair (left) and the ± 8 wave pair (right). As in Figure 1, the OPDs are shown with a linear intensity scale stretched over ± 200 nm.

J. Green (JPL), B. Dean (GSFC) et al.,
Proc. SPIE (Glasgow 2004)

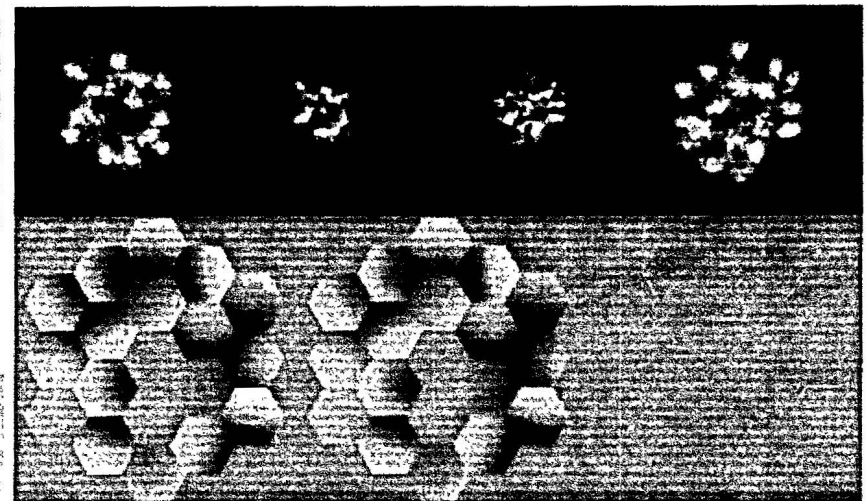


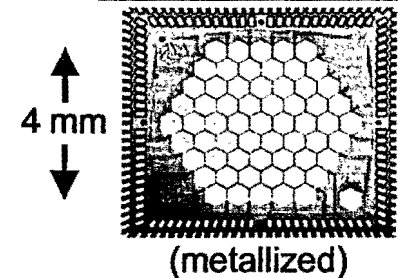
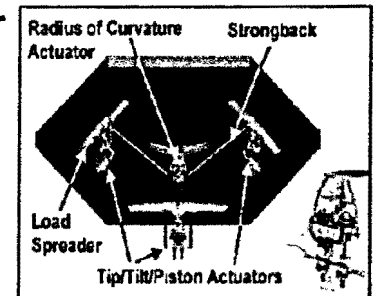
Figure 7. Fine phasing example. Top: simulated images with defocus values of $-6, -3, 3, 6$ waves PTV (log display). Lower left: the actual phase map (~ 250 nm rms). Lower center: estimated phase. Lower right: difference (~ 10 nm rms).

D.S Acton et al. (Ball Aerospace),
Proc. SPIE (Glasgow 2004)

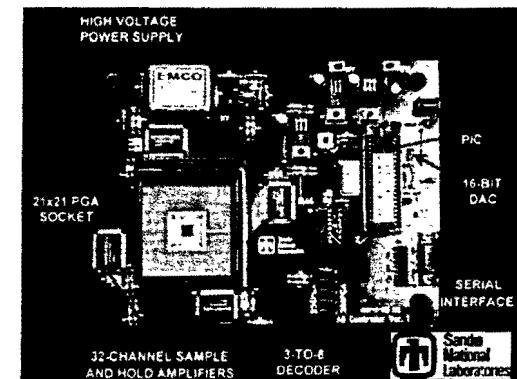
WFS at U of R WaveFront Sensing Improvements

- Develop improved WFS (phase retrieval) algorithms
 - Faster, converge more reliably, less sensitive to noise, 2π jumps
 - Work with larger aberrations, broadband illumination, jitter
 - Refining iterative transform, gradient search algorithms
 - Increase robustness and accuracy
 - Extended objects
 - Phase diversity
 - Phase retrieval performance

- Experiments with U of R telescope laboratory simulator
 - Adaptive optics MEMS deformable mirror
 - Interferometer measure wavefront independently
 - Put in misalignment, reconstruct wavefronts, compare with interferometer “truth”



- 61 piston/tilt hexagonal mirrors
- 497 μm diam. (polysilicon), 500 μm center-center
- 27 μm stroke
- 99% fill factor (polysilicon), 96% (metal)



- Phase Retrieval found the correct prescription for HST
 - Getting all the physics into the algorithm key to accuracy
 - Was not fully trusted by NASA
 - Hubble repair successful

- NASA has chosen phase retrieval for fine phasing of JWST
 - Key component in the system operational concept

Questions?